



Interpretation of multiple melting behaviour in poly (ether ether ketone) revisited: Two-dimensional correlation mapping approach

Abdul G. Al Lafi¹ · Ghina Alsayes¹

Received: 14 October 2020 / Accepted: 23 June 2021 / Published online: 10 July 2021
© Akadémiai Kiadó, Budapest, Hungary 2021

Abstract

Two-dimensional correlation mapping (2D-CM) is a newly developed analytical tool, which has been applied successfully to solve many problems in the field of analytical chemistry. It was used in the present work to analyse the differential scanning calorimetry (DSC) curves of different poly (ether ether ketone) (PEEK) samples. The use of 2D-CM enabled to correlate data from different DSC measurements and extract information related to the double melting behaviour of PEEK. In particular, the results indicated that the two main melting processes at 596.5 and 617.0 K represented two different crystal types. Thickening of crystals occurred only with the higher melting process, whilst the small size of crystals contributed to the lower melting enabled them to diffuse and melt at lower temperatures. Thermal stability and geometry characteristics of formed crystals were the driving force for the observed multiple melting behaviour. 2D-CM analysis provided a variety of advanced methods to correlate and analyse DSC data and made extracting conclusions straightforward.

Keywords Poly (ether ether ketone) · Crystallization · Double melting · DSC · Two-dimensional correlation mapping

Introduction

Differential scanning calorimetry (DSC) is a useful technique in the field of polymer characterization. It has been utilized to investigate the response of polymers to heating/cooling to determine their thermal properties including melting and crystallization processes as well as the glass transition temperature [1]. It has been also used to measure heat capacities and enthalpies of solid–solid transitions such as those observed in primary alkylamides [2]. Recently, the application of two-dimensional correlation mapping (2D-CM) has been proposed to analyse the data obtained by the DSC operating on both dynamic and isothermal modes [3, 4]. The concept of 2D-CM has been applied successfully to analyse low-temperature DSC data to investigate the molecular interaction and the effect of both cross-linking and ion-exchange capacity on the state of water in sulfonated poly (ether ether ketone) (SPEEK) [3], the thermal properties of which have been given a growing attention [5]. Moreover, 2D-CM approach has been utilized to analyse DSC rate–time

data in the isothermal crystallization of poly (ether ether ketone) (PEEK) [4]. The main result of the 2D-CM analysis was the identification of an overlap between the primary (Avrami-like) crystallization and a secondary crystallization process, an effect that is known for over 60 years [6]. Although this overlap can also be easily found using conventional curve analysis, 2D-CM was useful in kinetic crystallization rate studies as it clearly indicated that the n value was changing with temperature, and this was conclusive evidence for primary and secondary crystallization being present. It has been shown that secondary crystallization is diffusion controlled and its rate increases with increasing temperature [7]. Accordingly, its contribution to the overall crystallinity must increase as its rate increases and the primary crystallization slows down. That is why the ability of the DSC to detect secondary crystallization increased towards the end of primary crystallization. This sensitivity becomes less and less with decreasing the supper cooling [8]. K. Philipson et al. showed that the secondary crystallization could be visualized after $X_p=0.9$ with DSC but after $X_p=0.4$ with more sensitive technique such as Fourier transformation infra-red spectroscopy (FTIR) [9]. An improvement in resolution when FTIR was used. However, the correlation peaks started in the 2D-CM-DSC maps as low as $X_p=0.2$ and lower indicating the co-occurrence of both primary and

✉ Abdul G. Al Lafi
cscientific9@aec.org.sy

¹ Department of Chemistry, Atomic Energy Commission, P.O. Box: 6091, Damascus, Syrian Arab Republic

secondary crystallization. In addition, the finding of 2D-CM was consistent with the new series of isothermal crystallization analysis based on the modification of Avrami equation, which has been initiated by James N. Hay [10]. The new model has resulted in many publications covering different type of polymers [11, 12]. All of that strengthens the scientific merits of 2D-CM-DSC and encourages the authors to investigate another issue, which is related to the multiple melting behaviour encountered with many polymers, such as PEEK [8, 13–15]. Two hypotheses have been suggested as the origin of this phenomenon namely: two separate crystal morphologies and recrystallization effects.

In the present work, the DSC behaviour of PEEK samples was measured under different conditions focusing on the effect of heating/cooling rates, crystallization time and temperature on the multiple melting peaks. The collected data were analysed by the 2D-CM approach to investigate the capability of this relatively new analytical tool in determining the origin of melting multiplicity in PEEK.

Experimental

Materials and differential scanning calorimetry (DSC)

Amorphous PEEK was obtained from Goodfellow Ltd., the United Kingdom, as 100- μ m-thick films with a density of 1260 kg m⁻³. A PerkinElmer differential scanning calorimeter, DSC-2, equipped with a water-cooled jacket and interfaced to a computer was used to record the DSC curve of PEEK. All measurements were carried out under argon with a flow of 20 cm³ min⁻¹ following the procedure developed elsewhere [6, 16]. PEEK samples (7.5 mg) were cut to fit the shape of the aluminium pans used to encapsulate the sample precisely, and an empty pan was used as a reference. All samples were initially heated to 650 K at 320 K min⁻¹ and held at this temperature for 5 min to clear previous thermal history. Each set of samples was then subjected to different type of thermal history before measuring the DSC curve, and this will be mentioned in the appropriate place in the paper. Temperature and enthalpy calibrations were performed with ultra-pure metal standards: indium (melting point, m.pt: 429.78 K, $\Delta H = 29.2$ J g⁻¹), tin (m.pt: 505.06 K) and lead (m.pt: 600.65 K).

Data pre-treatments and 2D-CM analysis

All the DSC heat flow–temperature curves were baseline corrected, which was recorded with the same thermal program for each set of PEEK samples using two empty aluminium pans. The data were then smoothed with a Savitzky–Golay smoothing method using a second-order polynomial function

with 15 points as the number of the points of the convolution weights (to reduce noise) and finally, normalized based on sample mass. Other data pre-treatments will be discussed in appropriate place in the paper. Subsequent 2D correlation analyses were performed using the algorithm developed by Noda [17, 18] and calculated using the 2D-Shige version 1.3 software (Shigeaki Morita, Kwansei-Gakuin University, 2004–2005). The perturbation variable was chosen according to the experiment, and heating rate, crystallization time as well as cooling rate were all considered. Sets of data were represented as a matrix wherein each row is comprised of the heat flow at a given temperature, and each column corresponds to the heat flow at a specific perturbation for different temperatures. The reference DSC curve was taken as the heat flow response corresponding to the lowest perturbation unless otherwise stated.

Results and discussion

The effect of crystallization temperature on melting

Figure 1a shows an example of the DSC curve for two PEEK samples, samples A and B that were scanned from 350.0 and 586.3 K, respectively, to 650.0 K at 20 K min⁻¹. As can be seen, another lower melting peak appeared in sample B.

Samples of PEEK were melted at 650.0 K for 5 min, cooled at 80 K min⁻¹ and held isothermally for extended time ranging from 10 to 60 min (depending on the holding temperature to insure complete crystallization). After that time, a heating scan was recorded from the holding temperature to 650.0 K at 20 K min⁻¹. The overall results are presented in Fig. 1b in a plot of the melting temperatures as a function of the holding temperature. Holding below the melting point at any temperature above T_g , introduced a second lower melting process. Both melting peaks' temperatures were observed to increase with increasing holding temperature, but the lower melting temperatures were a linear function of the crystallization temperatures whilst a change on the slope around 566.8 K was observed with the higher melting peaks. Chen and Chung analysed crystallization using an optical microscopy, and they concluded that PEEK exhibited regime II to III transition at 569.0 ± 1.0 K [19, 20].

In fact, heating at 20 K min⁻¹ means that the sample will stay at a specific temperature for no more than 3 s, which is less than the time required for the formation of crystal. This is why the first melting peak did not appear in sample PEEK-A. When starting the experiment from 586.3 K, the DSC will hold the sample for 1 min before the dynamic section starts and as a result allow some crystal to form and participate in the lower melting peak. It is expected that the minimum time needed for the appearance of the first melting

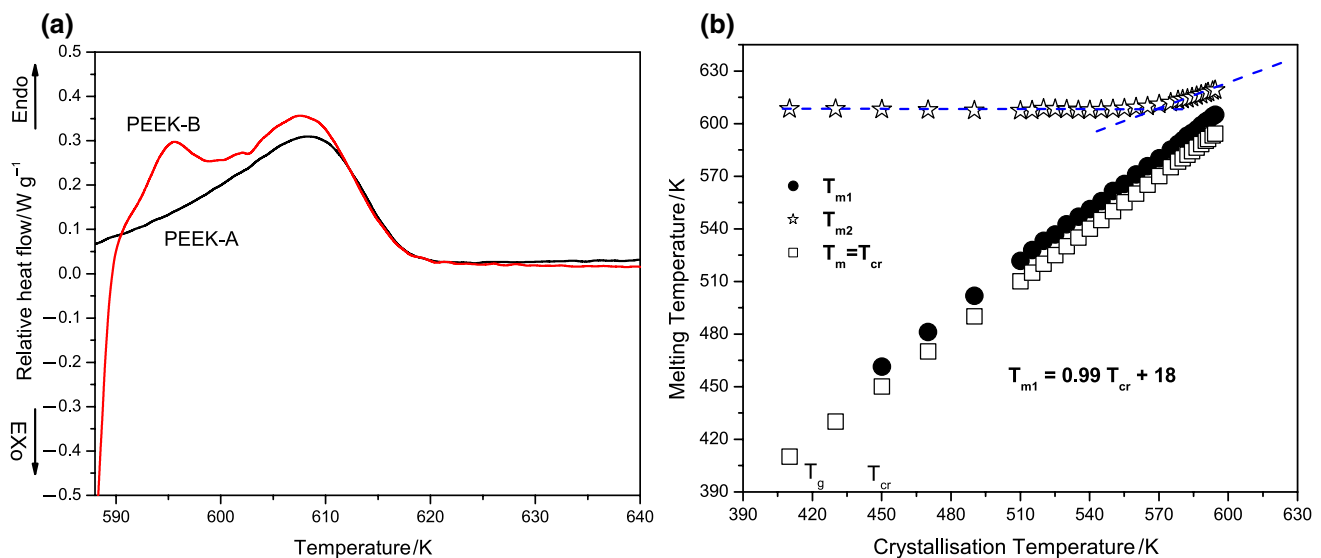


Fig. 1 **a** DSC curves of PEEK samples, and **b** The dependence of the melting temperatures of PEEK on crystallization temperature

point will vary with holding temperatures, as there would be nucleation stability and activation energy considerations. It should be noted that the lower melting point did not obey Hoffman and Weeks procedure [21], and thus, there were no effects of crystal thickness on this endotherm.

The effect of heating rate on melting peaks

Samples of PEEK were heated to 586.3 K at different heating rates and then, were scanned to 650.0 at 20 K min⁻¹. It was observed that the first melting peak sharpens with decreasing heating rate, but the peak temperatures were nearly constant, see Fig. 2. It was difficult to separate the two peaks and calculate the area under each one; however, Fig. 2 shows that the area under the second melting curves decreased with decreasing heating rate and that of the first melting increased. This may imply that there was a transformation from one region to another.

2D-CM-DSC was applied to analyse the data in Fig. 2 by normalizing the curves based on the total area under each of them and subtracting a reference DSC curve, which was taken as the DSC curve at the maximum heating rate used, i.e. at 320 K min⁻¹. The results of this procedure are depicted in Fig. 3.

In the synchronous map of Fig. 3a, there were three auto-peaks at 594.5, 600.0 and 608.5 K, and a positive cross-peak at (608.5, 594.5) K, which indicated that both melting processes changed in the same direction with increasing heating rate. This suggested that the process occurred simultaneously. In the asynchronous map of Fig. 3b, there were two cross-peaks, one of which was positive that correlated the signals at (612.5, 606.5) K and the other was negative that correlated the signals at (608.5, 594.5) K. The signs of

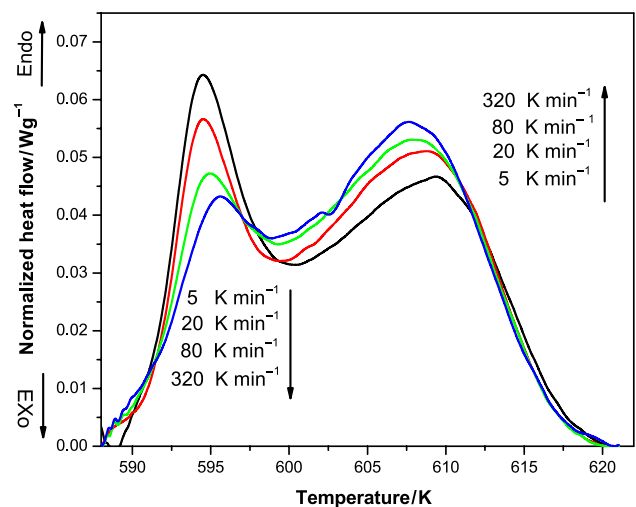


Fig. 2 The effect of heating rate on melting behaviour of PEEK

cross-peaks indicated that the lower melting process increase occurred before the higher melting process. This implied the presence of a bimodal population of crystals present at the beginning of the heating scans [13]. The low endotherm was attributed to the melting of lower stability crystals, whilst the higher endothermic region was associated with the melting of the most stable crystals.

The appearance of correlation peak at 612.7 K may imply the thickening of the crystal with decreasing heating rate as this temperature corresponded to the end of second melting peak. According to the 2D-CM, there was a multiple melting behaviour and at least three processes were identified at 594.5, 600.0 and 608.5 K, whilst only two of them were detectable by conventional DSC. Marand et al. [13] showed

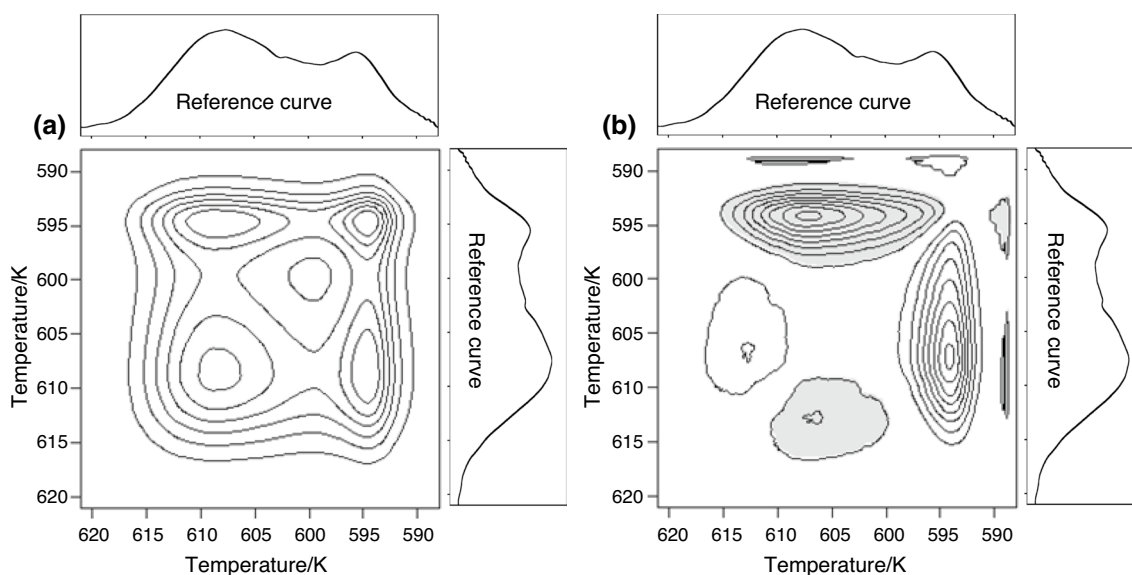


Fig. 3 The 2D-CM analysis of the data in Fig. 2: **a** synchronous and **b** asynchronous maps

that care must be paid to analyse such effects on the DSC and a special correction procedure had to be applied on the data. They had observed that the heating rate dependence of the lower melting process was identical for melt- and cold-crystallized PEEK samples, whilst the higher melting process was different for the two series of samples. In addition, the presence of an intermediate melting process whose associated latent heat increased with heating rate at the expense of the highest endotherm was observed.

Many processes contribute to the complicated melting process of polymeric crystals. These are reorganization, annealing, or recrystallization on heating before final melting. On heating, the crystal phase can be perfected and their lamellae can thicken which increases the measured melting temperature with decreasing heating rate. However, in the case of a large extended-chain crystal of nylon 6, the measured melting temperature decreased with decreasing heating rate [22].

In conclusion: the results of 2D-CM-DSC were in line with the reported results and provided the advantages of: (I) obtaining a consistent results without using any correction method apart from the data pre-treatment which is necessary for 2D-CM, and (II) showing the multiplicity in the DSC curves.

The effect of crystallization time on melting process

PEEK samples were melted at 650.0 K, cooled to 586.3 K at 80 K min^{-1} and crystallized for time varied from 5 to 40 min. The melting curves were recorded after each run at 20 K min^{-1} . The results are depicted in Fig. 4. It was noted that the higher endotherm started before the lower one and

both endotherms increased with increasing crystallization time.

The peak temperature of the higher melting appeared to be constant during crystallization as depicted in Fig. 5a, but the total area increased with time and did not reach a constant value even after a complete crystallization experiment, see Fig. 5b. On the contrary, the lower melting temperatures peaks increased with time but slowed down after 25 min of crystallization.

2D-CM-DSC was also applied to analyse the data in Fig. 4 by normalizing the curves based on the total area under each of them and subtracting a reference DSC curve,

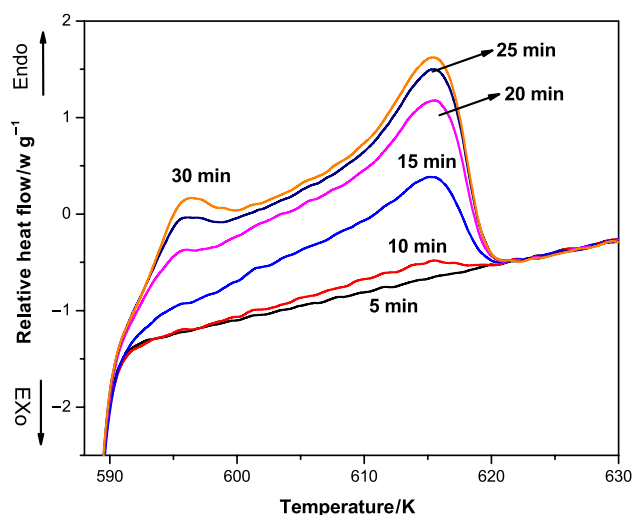


Fig. 4 DSC curves for PEEK samples during and after crystallization

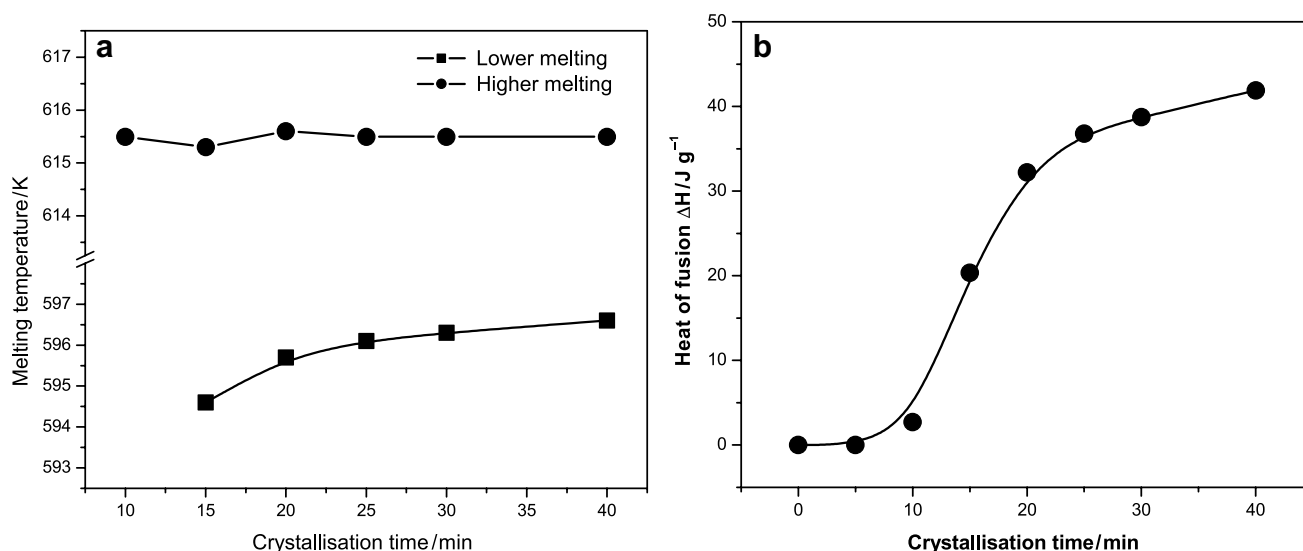


Fig. 5 The effect of crystallization time on **a** the melting temperature and **b** the heat of fusion ΔH_m

which was taken as the average DSC curve over all crystallization times. The results are depicted in Fig. 6.

The important features of the 2D-CM-DSC maps were considered. In the synchronous map of Fig. 6a, the most important auto-peaks located at 617.0 and 596.5 K corresponded to the higher and lower melting endotherms, respectively. The other auto-peaks that were observed in the temperature region from 600.0 to 615.0 K represented intermediate melting processes. There was also a positive cross-peak at (617.0, 596.5) K, which indicated that both melting temperatures increased with increasing crystallization time. On the other hand, the intermediate melting

processes correlated with negative signs with both the lower and the higher melting peaks. In the asynchronous map of Fig. 6b, there was a positive cross-peak at (617.0, 596.5) K. The signs of cross-peaks from both synchronous and asynchronous maps indicated that the higher melting process increase occurred before the lower melting process. In addition, all melting processes in the region 600.0–615.0 K change occurred before that of the two main melting at 595.5 and 617.0 K, which was indicative of transformation from the region 600.0–615.0 K to the other two main melting endotherms.

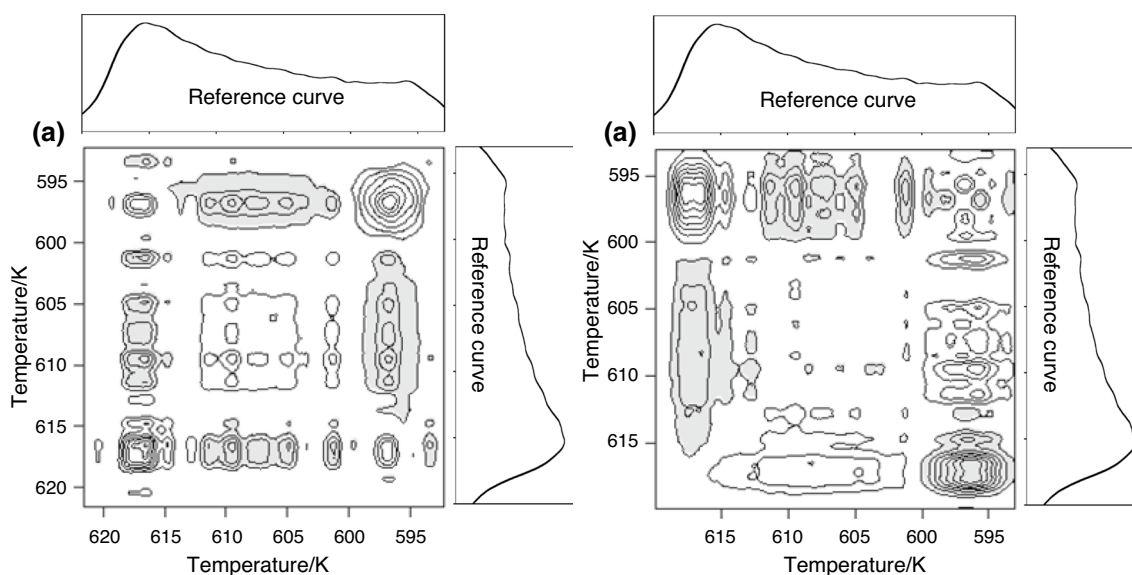


Fig. 6 The 2D-CM analysis of the data in Fig. 4: **a** synchronous and **b** asynchronous maps

The 2D-CM-DSC results could be explained by assigning the temperature region from 600.0–615.0 K to the melting and recrystallization of crystals of different stabilities. Part of these crystals continued growth and form stable crystals that contributed to the higher melting endotherm at 617.0 K. The remaining part broken down and forms less stable crystals that contributed to the lower endotherm at 596.5 K.

The previous discussion was consistent with 1D-DSC analysis discussed in Fig. 1b, as only the thicker crystals that obeyed Hoffman–Weeks equation contributed to the higher melting endotherms.

The effect of crystallization time on recrystallization process

PEEK sample was melted at 650.0 K, held for 5 min, cooled to 586.3 K at 20 K min^{-1} and crystallized isothermally for extended time from 0.5 to 40 min. The cooling curves were recorded immediately after each isothermal crystallization run from the isothermal crystallization temperature, i.e. 586.3 K to room temperature at a cooling rate of 20 K min^{-1} . The recrystallization temperature shifted to higher values with increasing crystallization time, see Fig. 7a, and the heat flow decreased, see Fig. 7b. After 40 min of isothermal crystallization, no recrystallization peak was observed. It was evident that thickening of the crystals was not detectable by the DSC cooling scan. It was also evident that the induction period contributed to the recrystallization peak as the later decreased in heat flow and shifted to higher temperature before the primary crystallization started.

2D-CM-DSC was also applied to analyse the data in Fig. 7b after normalizing all curves based on the total area

and subtracting a reference DSC curve, which was taken as the DSC curve at the maximum isothermal crystallization time used, i.e. at 40 min. The results are depicted in Fig. 8.

The synchronous map, Fig. 8a, shows a characteristic angel pattern, comprising two positive auto-peaks at 555.5 and 565.5 K correlating to each other with two negative cross-peaks at (555.5, 565.5) and (565.5, 555.5) K. The auto-peak at 555.5 K was disproportionately large compared to the other auto-peak at 565.5 K, which arose from the difference in breadth of the two recrystallization processes, probably due to the different types of crystals.

The asynchronous map, Fig. 8b, shows the characteristic distorted butterfly pattern, consisting of a pair of elongated cross-peaks of opposing signs located very close to the diagonal and near the stronger auto-peak side, i.e. the peak at 555.5 K. Next to these elongated cross-peaks and slightly away from the diagonal, are another set of lower intensity cross-peaks [3, 18]. The patterns observed in both synchronous and asynchronous maps are characteristic of signals shift coupled with an intensity change, and the direction of the shift is determined by the signs of the asynchronous cross-peaks within the butterfly cluster as outlined by Noda [18]. The elongated cross-peak above the diagonal was positive, and that below the diagonal was negative, which indicated that the signal position was shifting from left to right along the horizontal axis of the 2D-CM map and from bottom to top along the vertical axis.

The 2D-CM patterns indicated that the recrystallization peaks shifted to higher temperatures and the total area decreased with increasing isothermal crystallization time. This was in agreement with the classical DSC analysis shown in Fig. 7 and further confirmed the applicability of

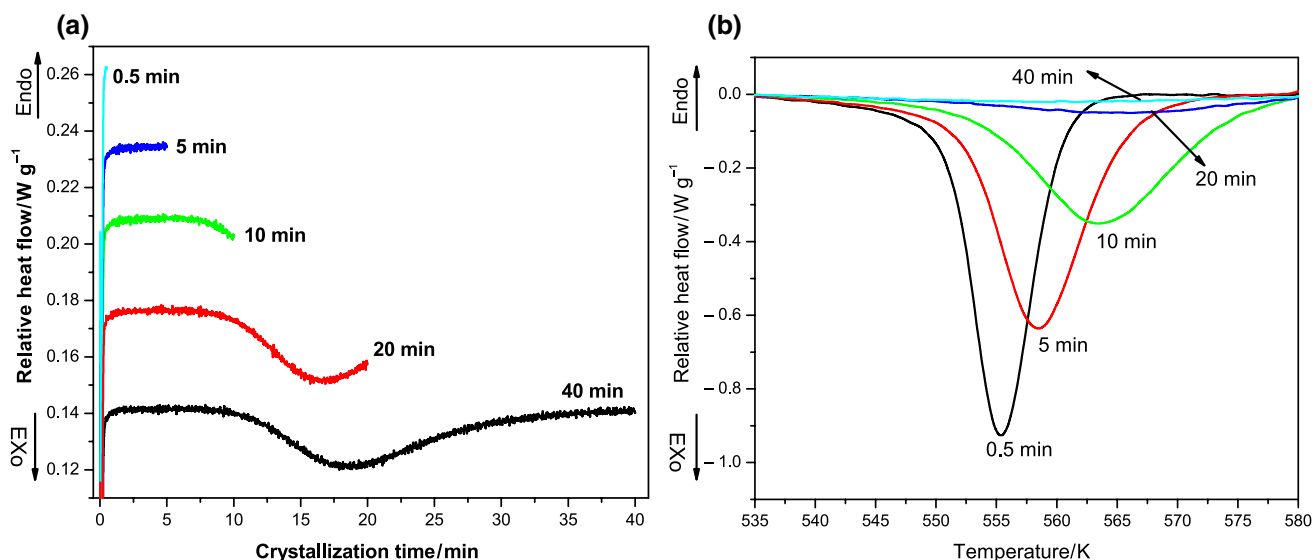


Fig. 7 DSC curves for PEEK sample **a** crystallized isothermally at 586.3 K for different times and **b** scanned to 350 K at a cooling rate of 20 K min^{-1}

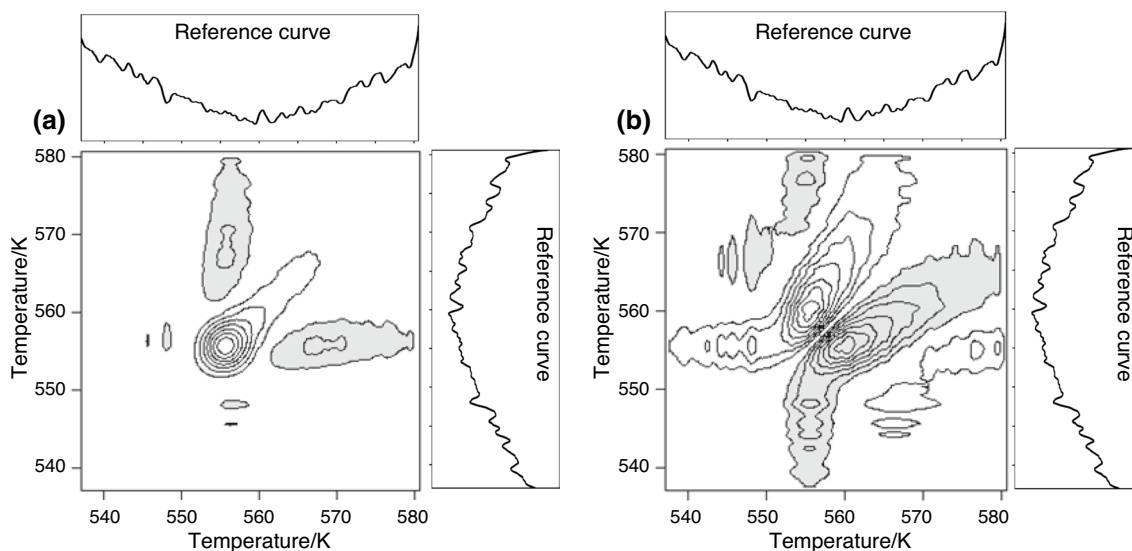


Fig. 8 The 2D-CM analysis of the data presented in Fig. 7b: **a** synchronous and **b** asynchronous maps

2D analysis to this type of DSC measurements. In addition, the 2D-CM results indicated different temperature dependency of the two different crystallization processes. This was consistent with literature [7], as it has been shown that secondary crystallization was diffusion controlled and its rate increased with increasing temperature. Thus, with increasing isothermal crystallization time the contribution of secondary crystallization to the overall crystallinity must increase as its rate increases and the primary crystallization slows down.

Hybrid-correlation approach

The data presented in Figs. 4 and 7 were collected under the same perturbation (isothermal crystallization time) but under different conditions (heating or cooling scans). In particular, by considering data generated from both heating and cooling scans of PEEK samples that were isothermally crystallized to the same time, the similarity and/or difference between the two sets of data could be explored by the use of the hybrid 2D approach [23–25]. The results are presented in Fig. 9 as the synchronous map, of which the y axis represents the portion of crystals remain after holding (secondary crystallization) and the x axis represents the melting of the crystallized portion (primary crystallization) of PEEK sample.

The important features of the hybrid 2D-CM were that the middle region, i.e. 600.0–610.0 K correlated with positive signs with the start and the end temperatures of the recrystallization process, but it correlated with negative signs with the middle recrystallization peak. This confirmed that this region, i.e. from 600.0 to 610.0 K contained crystals of different stabilities, which was consistent with the previous assignments. On the other hand, the negative sign indicated

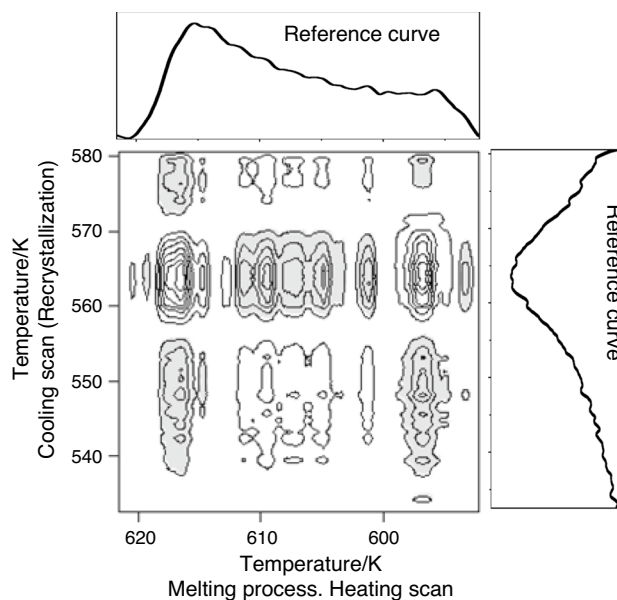


Fig. 9 The synchronous 2D-CM-DSC map of both heating and cooling scans after crystallization of PEEK for different time. A hybrid approach

different direction of change of the melting of crystal in the region 600.0–610.0 K and recrystallization peak temperature. The lower (at 596.5 K) and higher (at 617.0 K) melting processes correlated with the start and end temperatures of the recrystallization process with negative signs, but they correlated with positive signs with the middle recrystallization peak. This indicated that the recrystallization peak represented both contribution of crystals melted at 596.5 and 617.0 K, which was consistent with Fig. 7 as the recrystallization peak shifted and the area decreased before the

isothermal crystallization took place. In conclusion, the 2D-CM-DSC confirmed again the presence of two different types of crystals.

Conclusions

Two-dimensional correlation mapping (2D-CM) was used to analyse the differential scanning calorimetric curves of different PEEK samples, to investigate the multiple melting behaviours. One obvious merit of 2D-CM analysis is that it enabled different experimental data to be correlated with each other and open the way of new information extraction procedures. Many affecting factors were thus considered, in particular the heating rate, crystallization time and temperature. Generalized and hybrid 2D-CM approaches were used to analyse the different data sets obtained, and the overall results suggested that the origin of multiple melting in PEEK was the presence of two different type of crystals that have different temperature dependency. 2D-DSC-CM has been shown to be a versatile data tool analysis and valuable information extraction method. Thus, it would be advantageous analytical procedure in polymer science and analysis.

Acknowledgements The authors thank Prof. I. Othman; the Director General of the Atomic Energy Commission of Syria, and Prof. A. W. Allaf the Head of Chemistry Department for their support. Thanks are also due to Prof. J. N. Hay for his useful discussions.

Authors' contributions Conceptualization, formal analysis, writing—original draft, were contributed by AGAL. Investigation and visualization were contributed by GA.

Funding This study was funded by [Atomic Energy Commission of Syria (AECS)].

Declarations

Conflicts of interest The authors declare that they have no conflicts of interest.

References

- Ferguson HF, Frurip DJ, Pastor AJ, Peerey LM, Whiting LF. A review of analytical applications of calorimetry. *Thermochim Acta*. 2000;363:1–21.
- Abate L, Badea E, Blanco I, Gatta GD. Heat capacities and enthalpies of solid–solid transitions and fusion of a series of eleven primary alkylamides by differential scanning calorimetry. *J Chem Eng Data*. 2008;53:959–65.
- Al-Lafi AG, Hay JN. State of the water in crosslinked sulfonated poly(ether ether ketone) two-dimensional differential scanning calorimetry correlation mapping. *Thermochim Acta*. 2015;612:63–9.
- Al-Lafi AG, Hay JN. The isothermal crystallization of poly(ether ether ketone) by two-dimensional differential scanning calorimetry correlation mapping. *J Appl Polym Sci*. 2017;134:44378.
- Abate L, Blanco I, Orestano A, Pollicino A, Recca A. Evaluation of the influence of various (ether, ketone and sulfone) groups on the apparent activation energy values of polymer degradation. *Polym Degrad Stab*. 2003;80:333–8.
- Hay JN. Application of the modified Avrami equations to polymer crystallisation kinetics. *Br Polym J*. 1971;3:74–82.
- Phillipson K, Jenkins MJ, Hay JN. The ageing of poly(ϵ -caprolactone). *Polym Int*. 2015;64:1695–705.
- Wei C-L, Chen M, Yu F-E. Temperature modulated DSC and DSC studies on the origin of double melting peaks in poly(ether ether ketone). *Polymer*. 2003;44:8185–93.
- Phillipson K, Jenkins MJ, Hay JN. The kinetics of crystallization of poly(ϵ -caprolactone) measured by FTIR spectroscopy. *J Therm Anal Calorim*. 2016;123:1491–500.
- Hay JN. Secondary crystallization kinetics. *Polym Cryst*. 2018;1:e10007.
- Chen Z, Hay JN, Jenkins MJ. The effect of secondary crystallization on crystallization kinetics – Polyethylene terephthalate revisited. *Eur Polym J*. 2016;81:216–23.
- Aziz AA, Samsudin SA, Hay JN, Jenkins MJ. The effect of a secondary process on polymer crystallization kinetics – 3 Co-poly (lactic acid). *Eur Polym J*. 2017;94:311–21.
- Marand H, Alizadeh A, Farmer R, Desai R, Velikov V. Influence of structural and topological constraints on the crystallization and melting behavior of polymers 2 Poly(arylene ether ether ketone). *Macromolecules*. 2000;33:3392–403.
- Jenkins MJ, Hay JN, Terrill NJ. Structure evolution in melt crystallized PEEK. *Polymer*. 2003;44:6781–7.
- Ivanov DA, Legras R, Jonas AM. Interdependencies between the evolution of amorphous and crystalline regions during isothermal cold crystallization of poly(ether-ether-ketone). *Macromolecules*. 1999;32:1582–92.
- Al-Lafi AG, Hay JN, Parker DJ. The effect of proton irradiation on the melting and isothermal crystallization of poly(ether ether ketone). *J Polym Sci B: Polym Phys*. 2008;46:1094–113.
- Noda I. Generalized two-dimensional correlation method applicable to infrared raman, and other types of spectroscopy. *Appl Spectrosc*. 1993;47:1329–36.
- Noda I, Ozaki Y. Two-dimensional correlation spectroscopy: applications in vibrational and optical spectroscopy. Chichester: Wiley; 2004.
- Chen M, Chung CT. Analysis of crystallization kinetics of poly(ether ether ketone) by a nonisothermal method. *J Polym Sci B: Polym Phys*. 1998;36:2393–9.
- Chen M, Chen J-Y. Analysis of crystallization kinetics of poly(ether ether ketone). *J Polym Sci B: Polym Phys*. 1998;36:1335–48.
- Hoffman JD, Weeks JJ. Melting process and the equilibrium melting temperature of polychlorotrifluoroethylene. *J Res Nat bur Stand-A, Phys Chem*. 1962;66A:13–8.
- Piorkowska E, Rutledge GC, editors. Handbook of Polymer Crystallization. New Jersey: Wiley; 2013.
- Wu Y, Jiang J-H, Ozaki Y. A new possibility of generalized two-dimensional correlation spectroscopy: hybrid two-dimensional correlation spectroscopy. *J Phys Chem A*. 2002;106:2422–9.
- Wu Y, Meersman F, Ozaki Y. A novel application of hybrid two-dimensional correlation infrared spectroscopy: exploration of the reversibility of the pressure- and temperature-induced phase separation of Poly(N-isopropylacrylamide) and Poly(N-isopropylmethacrylamide) in aqueous solution. *Macromolecules*. 2006;39:1182–8.
- Al-Lafi AG, Rihawy MS. PIXE data analysis by two-dimensional correlation mapping techniques: analysis of chloride and sulfate ions attack in homemade mortar samples. *X-ray Spectrom*. 2020;49:379–89.

Publisher's Note Springer Nature remains neutral with regard to jurisdictional claims in published maps and institutional affiliations.